

Image enlargement based on the hyperbolic Coons interpolation

Juncheng Li*

Department of Mathematics and Econometrics, Hunan University of Humanities, Science and Technology, Dixing Road, Loudi, 417000, China

Received 1 March 2014, www.tsi.lv

Abstract

A method for image enlargement, making use of the hyperbolic Coons interpolation surface with shape parameters, is investigated in this paper. As a non-polynomial model, the hyperbolic Coons interpolation surface can represent the image better than the general interpolation methods. By altering the values of the shape parameters, the effects of image enlargement can be adjusted until achieving the satisfactory results. Experimental results show that the effects of image enlargement making use of the hyperbolic Coons interpolation surface are better than the general interpolation methods.

Keywords: image enlargement, hyperbolic Coons interpolation surface, shape parameters

1 Introduction

As an important part of image processing, image enlargement has been widely applied in different areas. Because a two-dimensional static grey image can be represented by a continuous function of two variables, surface interpolation methods are generally used to deal with image enlargement problems. The general interpolation methods for image enlargement include nearest interpolation, bilinear interpolation, bicubic interpolation, cubic spline interpolation, and so on [1, 2], which used polynomial models to construct image interpolation surfaces. However, the polynomials can only reflect the gradual change of data but not the mutability of data, the quality of the target images require to be further improved. Therefore, the uses of non-polynomial models would be better choices for constructing image interpolation surfaces.

Generally, curves and surfaces are established based on polynomial functions in Computer Aided Geometric Design (CAGD), in particular curve and surface design. Non-polynomial models, such as trigonometric or hyperbolic curves and surfaces, have gained very much interest in recent years within CAGD. Zhang constructed the C-Bézier curve and surface in the space $\{1, t, \sin t, \cos t\}$ [3]. Mainar and Chen defined the C-Bézier curves of higher order in the space $\{1, t, \dots, t^{k-3}, \cos t, \sin t\}$ [4, 5]. Wang constructed the non-uniform algebraic trigonometric B-splines in the space $\{1, t, \dots, t^{k-3}, \cos t, \sin t\}$ [6]. Han presented a cubic trigonometric Bézier curve with two shape parameters in the space $\{1, \sin t, \cos t, \sin^2 t\}$ [7]. Li constructed a class of quasi-cubic trigonometric curves in the space $\{1, \sin t, \cos t, \sin^2 t\}$ [8]. Liu presented another kind of trigonometric Bézier curve with two shape parameters in the space $\{1, \sin t, \cos t,$

$\sin^2 t\}$ [9]. Yan discussed a class of algebraic-trigonometric blended splines in the space $\{1, t, \sin t, \cos t, \sin^2 t, \sin^3 t, \cos^3 t\}$ [10]. Lü presented the hyperbolic polynomial B-splines in the space $\{\sinh t, \cosh t, t^{k-3}, t^{k-4}, \dots, t, 1\}$ [11], and Li extended these hyperbolic splines to the case of non-uniform knot vector [12]. Liu studied a kind of hyperbolic polynomial uniform B-spline surface with shape parameter in depth [13]. Li presented the hyperbolic polynomial Ferguson curve and Coons surface with shape parameters, which analogous to the corresponding cubic polynomial Ferguson curve and bicubic Coons surface [14].

Although the trigonometric and hyperbolic curves and surfaces have been widely studied, but up to now, the uses of the trigonometric or hyperbolic models for constructing interpolation surfaces in image processing have rarely been studied. The main purpose of this work is to investigate the use of the hyperbolic Coons interpolation surface with two shape parameters [14] to deal with image enlargement problems.

The present work is organized as follows. In Section 2, the basic principle of image zooming based on surface interpolation is given. In Section 3, the hyperbolic Coons interpolation surface is reviewed, and then image zooming making use of the hyperbolic Coons interpolation surface is investigated. In Section 4, the experimental results and discussion are provided. A short conclusion is given in Section 5.

2 The basic principle of image enlargement based on surface interpolation

The basic principle of image enlargement based on surface interpolation has two steps. The first step is to construct a continuous surface interpolating all the pixel

*Corresponding author e-mail: liuncheng82@126.com

points of the original image, and the second step is to obtain the target image by resampling the interpolation surface according to the enlargement ratio.

Given a grey image $I(x, y)$ with the size of $M \times N$, and $g_{i,j}$ ($i=0,1,\dots,M-1$; $j=0,1,\dots,N-1$) is the grey value with row i and column j according to the point (i, j) in the pixel plane. For enlarging the original image $I(x, y)$ to the target image $I'(x, y)$ with the size of $M_1 \times N_1$, firstly the continuous interpolation surface $F(x, y)$ ($0 \leq x \leq M-1$, $0 \leq y \leq N-1$) of the original image is constructed by some interpolation methods, then the target image can be obtained by uniform selecting $M_1 \times N_1$ pixel points in the interpolation surface $F(x, y)$. Therefore, the grey value g'_{i_1, j_1} with row i_1 and column j_1 of the target image $I'(x, y)$ satisfies

$$g'_{i_1, j_1} = F\left(\frac{M}{M_1}i_1, \frac{N}{N_1}j_1\right), \tag{1}$$

$$\mathbf{p}(u, v) = \begin{bmatrix} F_0(u; \alpha) & F_1(u; \alpha) & G_0(u; \alpha) & G_1(u; \alpha) \end{bmatrix} \begin{bmatrix} \mathbf{p}_{00} & \mathbf{p}_{01} & \mathbf{p}_{v00} & \mathbf{p}_{v01} \\ \mathbf{p}_{10} & \mathbf{p}_{11} & \mathbf{p}_{v10} & \mathbf{p}_{v11} \\ \mathbf{p}_{u00} & \mathbf{p}_{u01} & \mathbf{p}_{uv00} & \mathbf{p}_{uv01} \\ \mathbf{p}_{u10} & \mathbf{p}_{u11} & \mathbf{p}_{uv10} & \mathbf{p}_{uv11} \end{bmatrix} \begin{bmatrix} F_0(v; \beta) \\ F_1(v; \beta) \\ G_0(v; \beta) \\ G_1(v; \beta) \end{bmatrix}, \tag{2}$$

where \mathbf{p}_{00} , \mathbf{p}_{01} , \mathbf{p}_{10} and \mathbf{p}_{11} are point vectors in the four corner points; \mathbf{p}_{u00} , \mathbf{p}_{u01} , \mathbf{p}_{u10} and \mathbf{p}_{u11} are directional derivatives of direction u ; \mathbf{p}_{v00} , \mathbf{p}_{v01} , \mathbf{p}_{v10} and \mathbf{p}_{v11} are directional derivatives of direction v ; \mathbf{p}_{uv00} , \mathbf{p}_{uv01} , \mathbf{p}_{uv10}

where $i_1 = 0, 1, \dots, M_1 - 1$; $j_1 = 0, 1, \dots, N_1 - 1$.

According to the process of image enlargement, the key step is to construct the continuous image interpolation surface. In the following discussion, the hyperbolic polynomial Coons interpolation surface with two shape parameters [14] will be adopted to deal with image enlargement problems.

3 Image enlargement making use of the hyperbolic coons interpolation surface

3.1 THE HYPERBOLIC COONS INTERPOLATION SURFACE

For two arbitrary real number α and β , $\alpha, \beta > 0$, $0 \leq u \leq \alpha$, $0 \leq v \leq \beta$, the hyperbolic Coons interpolation surface [14] can be expressed as:

and \mathbf{p}_{uv11} are mixed directional derivatives; $F_i(t; \delta)$, $G_i(t; \delta)$ ($i=0,1$; $t=u,v$; $\delta=\alpha,\beta$) are the hyperbolic Hermite basis functions defined as:

$$\begin{cases} F_0(t; \delta) = \frac{1}{2-2C+\delta S} \left((1-C+\delta S) - St + S \sinh t + (1-C) \cosh t \right) \\ F_1(t; \delta) = \frac{1}{2-2C+\delta S} \left((1-C) + St - S \sinh t - (1-C) \cosh t \right) \\ G_0(t; \delta) = \frac{1}{2-2C+\delta S} \left(-(S-\delta C) + (1-C)t + (1-C+\delta S) \sinh t + (S-\delta C) \cosh t \right) \\ G_1(t; \delta) = \frac{1}{2-2C+\delta S} \left(-(\delta-S) + (1-C)t - (1-C) \sinh t + (\delta-S) \cosh t \right) \end{cases}, \tag{3}$$

where $S := \sinh \delta$, $C := \cosh \delta$.

In order to use the hyperbolic Coons interpolation surface defined as Equation (2) to deal with image enlargement problems, we redefine the surface on the

fixed interval $[0,1] \times [0,1]$. Let $s = \frac{u}{\alpha}$ and $t = \frac{v}{\beta}$, the hyperbolic Hermite basis functions can be redefined as follows:

$$\begin{cases} F_0(s) = F_0(u; \alpha), \quad F_1(s) = F_1(u; \alpha), \quad G_0(s) = \frac{1}{\alpha} G_0(u; \alpha), \quad G_1(s) = \frac{1}{\alpha} G_1(u; \alpha) \\ F_0(t) = F_0(v; \beta), \quad F_1(t) = F_1(v; \beta), \quad G_0(t) = \frac{1}{\beta} G_0(v; \beta), \quad G_1(t) = \frac{1}{\beta} G_1(v; \beta) \end{cases}, \tag{4}$$

According to Equation (2) and Equation (4), the function of the hyperbolic Coons interpolation surface can be expressed as follows:

$$f(s,t) = [F_0(s) \quad F_1(s) \quad G_0(s) \quad G_1(s)] \begin{bmatrix} f_{00} & f_{01} & f_{t00} & f_{t01} \\ f_{10} & f_{11} & f_{t10} & f_{t11} \\ f_{s00} & f_{s01} & f_{sr00} & f_{sr01} \\ f_{s10} & f_{s11} & f_{sr10} & f_{sr11} \end{bmatrix} \begin{bmatrix} F_0(t) \\ F_1(t) \\ G_0(t) \\ G_1(t) \end{bmatrix}, \tag{5}$$

where $0 \leq s \leq 1$ and $0 \leq t \leq 1$.

interpolation surface defined as Equation (5) has the following properties at the endpoints:

By simple deduction, the hyperbolic Coons

$$\begin{cases} f(0,0)=f_{00}, & f(0,1)=f_{01}, & f(1,0)=f_{10}, & f(1,1)=f_{11} \\ \frac{\partial f(0,0)}{\partial s}=f_{s00}, & \frac{\partial f(0,1)}{\partial s}=f_{s01}, & \frac{\partial f(1,0)}{\partial s}=f_{s10}, & \frac{\partial f(1,1)}{\partial s}=f_{s11} \\ \frac{\partial f(0,0)}{\partial t}=f_{t00}, & \frac{\partial f(0,1)}{\partial t}=f_{t01}, & \frac{\partial f(1,0)}{\partial t}=f_{t10}, & \frac{\partial f(1,1)}{\partial t}=f_{t11} \\ \frac{\partial^2 f(0,0)}{\partial s \partial t}=f_{sr00}, & \frac{\partial^2 f(0,1)}{\partial s \partial t}=f_{sr01}, & \frac{\partial^2 f(1,0)}{\partial s \partial t}=f_{sr10}, & \frac{\partial^2 f(1,1)}{\partial s \partial t}=f_{sr11} \end{cases} \tag{6}$$

Remark 1: Equation (6) shows that the hyperbolic Coons interpolation surface defined as Equation (5) has the same interpolation properties to the general bicubic polynomial Coons surface. However, the shape of the general bicubic polynomial Coons surface can not be adjusted when the boundary conditions are kept unchanged, while the shape of the hyperbolic Coons interpolation surface defined as Equation (5) can be easily adjusted by altering the value of the two shape parameters α and β . Given the boundary conditions

The effects on shape of the hyperbolic Coons interpolation surface by altering the value of α and β are shown in Figure 1, where (a) is generated by setting $\alpha=1$ and $\beta=5$, (b) is generated by setting $\alpha=2$ and $\beta=10$, (c) is generated by setting $\alpha=5$ and $\beta=1$, (d) is generated by setting $\alpha=10$ and $\beta=2$.

are:

$$\begin{bmatrix} f_{00} & f_{01} & f_{t00} & f_{t01} \\ f_{10} & f_{11} & f_{t10} & f_{t11} \\ f_{s00} & f_{s01} & f_{sr00} & f_{sr01} \\ f_{s10} & f_{s11} & f_{sr10} & f_{sr11} \end{bmatrix} = \begin{bmatrix} 0 & 0 & 0 & 0 \\ 0 & 0 & 0 & 1 \\ 1 & 1 & 1 & 1 \\ 0 & 1 & 1 & 1 \end{bmatrix}.$$

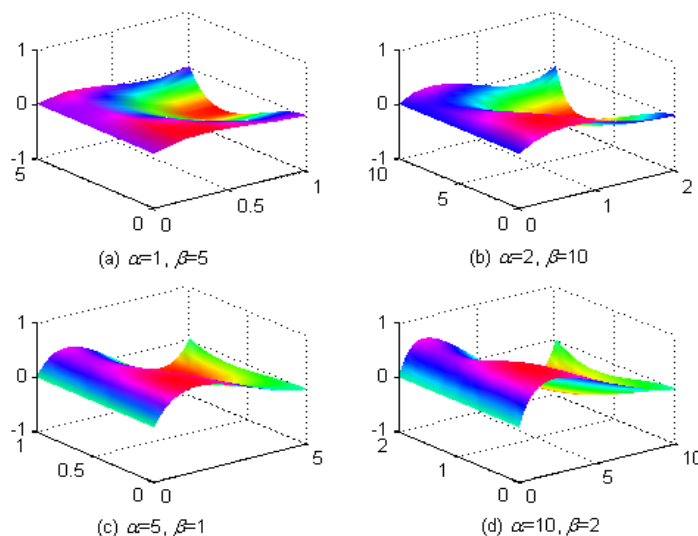


FIGURE 1 The hyperbolic Coons interpolation surfaces with different shape parameters

3.2 IMAGE ENLARGEMENT METHOD

Considering the region: $\Delta_{ij} = \{(x, y) | i \leq x \leq i+1, j \leq y \leq j+1\}$, $(i=0,1,\dots,M-2; j=0,1,\dots,N-2)$ in the pixel plane of

the original image $I(x, y)$.

Let $s = x - i$ and $t = y - j$, according to Equation (5) and Equation (6), the image interpolation surface in Δ_{ij} can be expressed as follows:

$$f_{ij}(s, t) = [F_0(s) \quad F_1(s) \quad G_0(s) \quad G_1(s)] \begin{bmatrix} a_{11} & a_{12} & a_{13} & a_{14} \\ a_{21} & a_{22} & a_{23} & a_{24} \\ a_{31} & a_{32} & a_{33} & a_{34} \\ a_{41} & a_{42} & a_{43} & a_{44} \end{bmatrix} \begin{bmatrix} F_0(t) \\ F_1(t) \\ G_0(t) \\ G_1(t) \end{bmatrix}, \tag{7}$$

where a_{mn} ($m, n = 1, 2, 3, 4$) satisfy:

$$\begin{cases} a_{11} = g_{i,j}, & a_{12} = g_{i,j+1}, & a_{13} = g_{i,j+1} - g_{i,j}, & a_{14} = g_{i,j+2} - g_{i,j+1}, \\ a_{21} = g_{i+1,j}, & a_{22} = g_{i+1,j+1}, & a_{23} = g_{i+1,j+1} - g_{i+1,j}, & a_{24} = g_{i+1,j+2} - g_{i+1,j+1}, \\ a_{31} = g_{i+1,j} - g_{i,j}, & a_{32} = g_{i+1,j+1} - g_{i,j+1}, & a_{33} = a_{34} = a_{43} = a_{44} = 0, \\ a_{41} = g_{i+2,j} - g_{i+1,j}, & a_{42} = g_{i+2,j+1} - g_{i+1,j+1}, & i = 0, 1, \dots, M-2; j = 0, 1, \dots, N-2 \end{cases}$$

and set $g_{i,N} = 2g_{i,N-1} - g_{i,N-2}$, $g_{M,j} = 2g_{M-1,j} - g_{M-2,j}$.

Remark 2: In order to get Equation (7), we use forward difference quotient to instead derivative and take the torsional vector of each corner point as zero. From Equation (7), the entire interpolation surface $F(x, y)$ of the original image $I(x, y)$ can be expressed as:

$$F(x, y) = f_{i,j}(s, t), \tag{8}$$

where $s = x - i$, $t = y - j$, $i \leq x \leq i+1$, $j \leq y \leq j+1$.

According to Equation (8), the entire image interpolation surface $F(x, y)$ ($0 \leq x \leq M-1, 0 \leq y \leq N-1$) is connected by $(M-1) \times (N-1)$ pieces of hyperbolic Coons interpolation surfaces and satisfies C^1 continuous.

For enlarging $I(x, y)$ to the target image $I'(x, y)$

with the size of $M_1 \times N_1$, let $x = \frac{M}{M_1} i_1$ and $y = \frac{N}{N_1} j_1$,

according to Equation (8), then $i = \lfloor x \rfloor$, $j = \lfloor y \rfloor$, where $\lfloor \cdot \rfloor$ is the round down functions.

Taking $s = x - i$ and $t = y - j$ into Equation (7), the grey values of the target image $I'(x, y)$ can be obtained by $g'_{i_1, j_1} = f_{i,j}(s, t)$, where $i_1 = 0, 1, \dots, M_1 - 1$; $j_1 = 0, 1, \dots, N_1 - 1$.

Remark 3: In contrast with the general interpolation methods, the use of hyperbolic Coons interpolation surface for constructing the image interpolation surface has the following advantages:

- 1) As a non-polynomial model, the hyperbolic polynomial not only can reflect the gradual change of data, but also can reflect the mutability of data;
- 2) The hyperbolic Coons interpolation surfaces directly interpolate the pixel points of the image, which avoiding solving a matrix system;
- 3) The hyperbolic Coons interpolation surface has two shape parameters α and β , the local characteristics of the target image can be proper adjusted by altering the two shape parameters.

4 Experimental results and discussions

The six images shown in Figure 2 are used as examples. In Figure 2, the size of (a) to (c) is 300×400 (8 bit) and the size of (d) to (f) is 256×256 (8 bit).

The effect of image enlargement is quantitatively compared by the PSNR (dB), which is defined as follows,

$$\text{PSNR} = 10 \times \log \frac{255^2}{\text{MSE}},$$

$$\text{MSE} = \frac{1}{M \times N} \sum_{i=1}^M \sum_{j=1}^N [I(i, j) - I'(i, j)]^2, \tag{9}$$

where $I(i, j)$ and $I'(i, j)$ is the original image and the target image respectively, $M \times N$ represents the size of the original image.

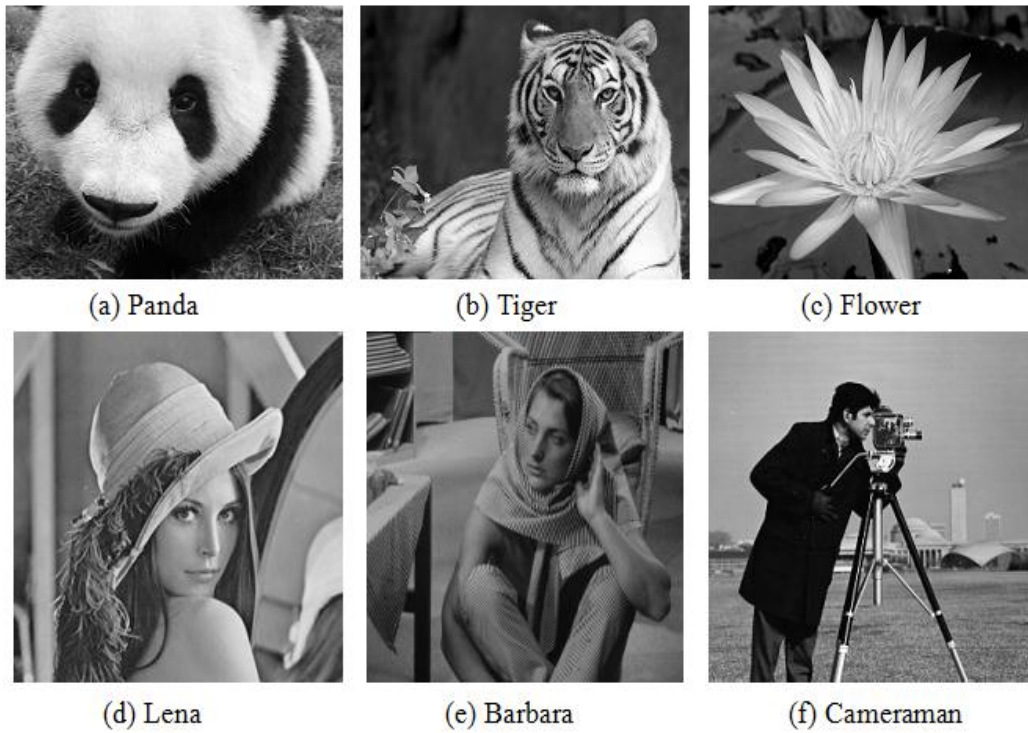


FIGURE 2 Original images for experiment

4.1 INFLUENCE OF THE SHAPE PARAMETERS ON IMAGE ENLARGEMENT

Firstly, in order to illustrate the effectiveness of the proposed method, we enlarge part of the Panda image (right part with the size of 100×60) shown in Figure 2

with 2 times and 3 times respectively. The enlarged images are shown in Figure 3, where the shape parameters of the image interpolation surface are set for $\alpha = \beta = 300$.

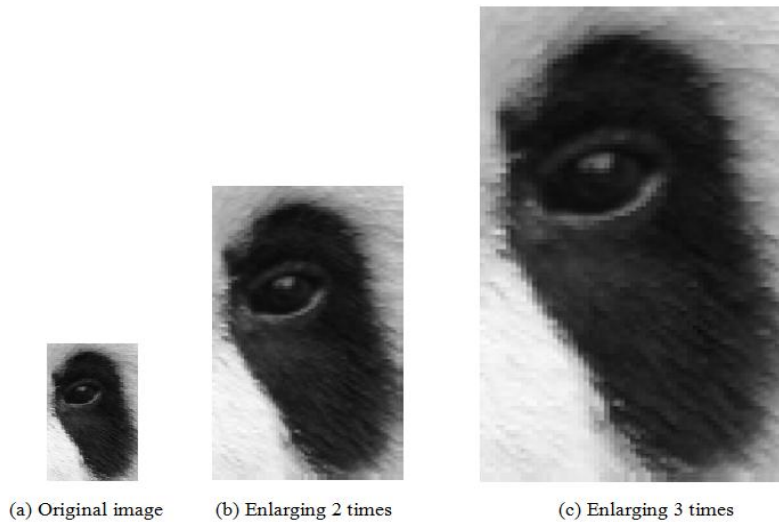


FIGURE 3 Experimental results of part of the Panda image

Figure 3 shows that the enlarged image does not appear obviously mosaic phenomenon and block phenomenon, and keep the edge information well. Even when the magnification is higher, the enlarged images still have good visual effects.

Secondly, we enlarge part of the Tiger image (face

part with the size of 100×100) shown in Figure 2 with 3 times. The enlarged images, when the two shape parameters are of different values, are shown in Figure 4.

The edge detection of the images in Figure 4 using the Prewitt operator (the threshold is set for 0.1) are shown in Figure 5.

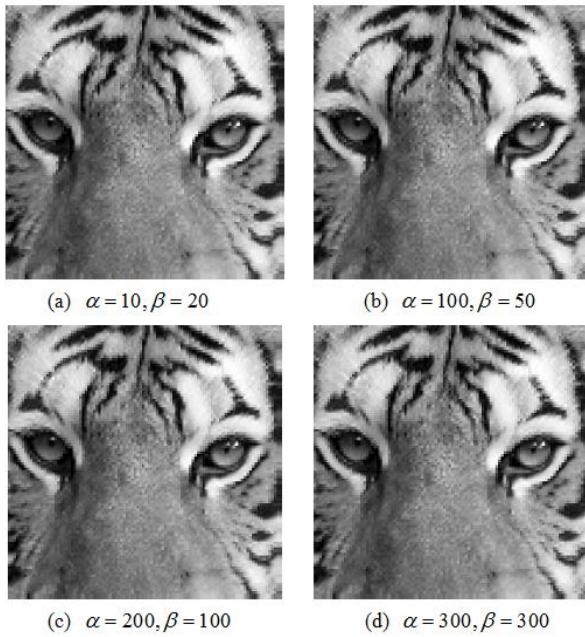


FIGURE 4 Experimental results of part of the Tiger image

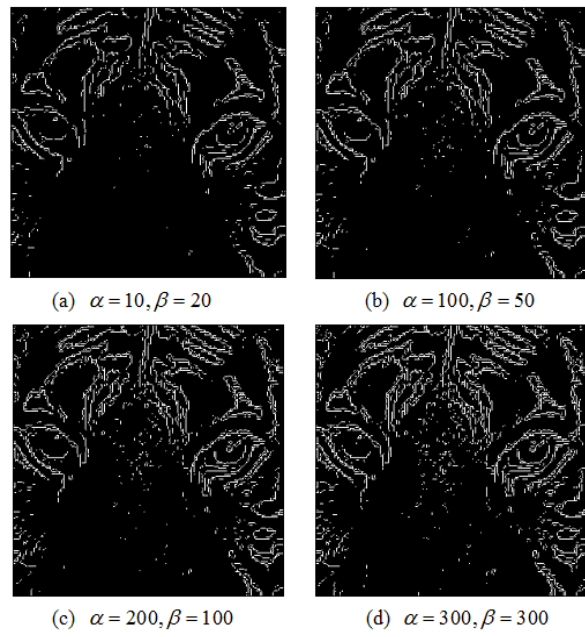


FIGURE 5 Edge detection of the images in Figure 4

Figure 4 and Figure 5 show that, when increasing the values of shape parameters α and β , the enlarged images would have gradually clear edge profile and boundary.

Remark 4: Through a large number of experiments on different images, we find that the shape parameter α and β have great influence on image enlargement. In general, the values of the shape parameters are greater, the better the effects of image enlargement. However, when the values of the shape parameters are too large, the enlarged images will produce certain distortion. So, in practical applications, the values of the shape parameters can be selected appropriately at first, if the target images are not satisfactory, we can modify the values of the shape parameters until obtaining satisfactory target

images.

4.2 COMPARISON OF THE PROPOSED METHOD WITH THE GENERAL METHODS

In order to compare the effects of image enlargement between the proposed method and the general interpolation methods, we firstly reduce the Flower image shown in Figure 2 under four minification using the bilinear interpolation, then enlarge the contractible images under four times again using the proposed methods (the shape parameters are set $\alpha = \beta = 300$) and the general interpolation methods respectively. Experimental results of the Flower image using different methods are shown in Figure 6.

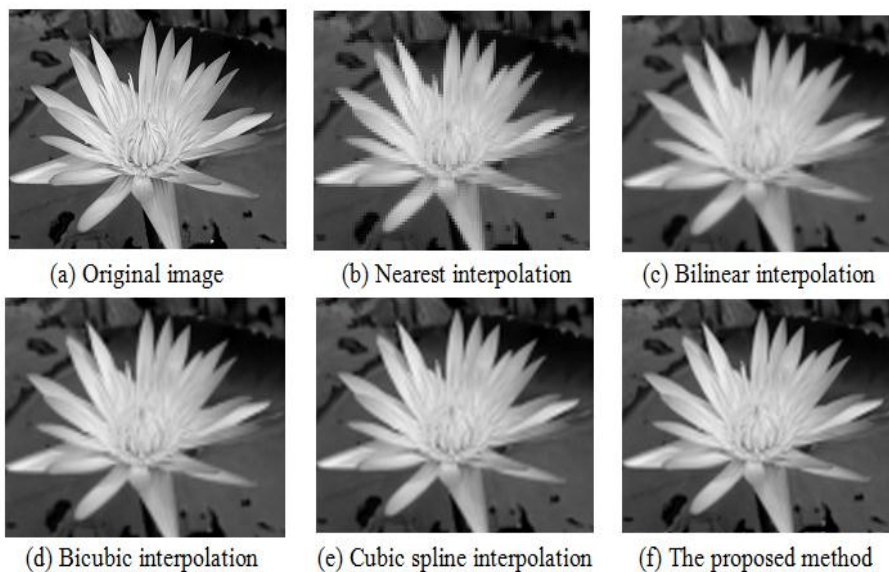


FIGURE 6 Experimental results of Flower image

Figure 6 shows that the proposed method can get better visual effect than the four general interpolation methods.

For quantitatively comparing the effects of image enlargement between the proposed method and the general interpolation methods, we firstly reduce the three original images shown in Figure 2(d)~(f) under four minification using bilinear interpolation, then enlarge the contractible images under four times again using the proposed methods (the shape parameters are set $\alpha = \beta = 300$) and the general interpolation methods respectively. The PSNR is computed to evaluate every method, which is listed in Table 1.

TABLE 1 The PSNR of different interpolation methods

Method	PSNR (dB)		
	Lena	Barbara	Cameraman
Nearest interpolation	32.4601	31.0211	33.0331
Bilinear interpolation	32.7356	31.2772	32.7071
Bicubic interpolation	33.2165	31.6113	32.9770
Cubic spline interpolation	33.3041	31.6939	32.9835
The proposed method	33.8866	32.0870	33.7275

References

- [1] Castleman K-R 1995 *Digital Image Processing*. New Jersey: Prentice Hall
- [2] Gonzalez R-C, Woods R-E 2005 *Digital Image Processing Using Matlab* New Jersey: Prentice Hall
- [3] Zhang J W 1999 *Graphical Models and Image Processing* **61**(1) 2-15
- [4] Mainar E, Pena J M 2002 *Computer Aided Geometric Design* **19**(4) 291-5
- [5] Chen Q Y, Wang G Z A 2003 *Computer Aided Geometric Design* **20**(1) 29-39
- [6] Wang G Z, Chen Q Y, Zhou M H 2004 *Computer Aided Geometric Design* **21**(2) 193-205
- [7] Han X-A 2009 *Applied Mathematics Letters* **22**(2) 226-31
- [8] Li J C, Zhao D B, Li B J, Chen G H A 2010 *Journal of Information and Computational Science* **7**(13) 2847-54
- [9] Liu H Y, Li L, Zhang D M 2011 *Journal of Information and Computational Science* **8**(7) 1217-23
- [10] Yan L L, Liang J F 2011 *Journal of Computational and Applied Mathematics* **235**(6) 1713-29
- [11] Lü Y G, Wang G Z, Yang X N 2002 *Computer Aided Geometric Design* **19**(6) 379-93
- [12] Li Y J, Wang G Z 2005 Two Kinds of B-Basis of the Algebraic Hyperbolic Space *Journal of Zhejiang University SCIENCE A* **6**(7) 750-9 (in Chinese)
- [13] Liu X M, Xu, W X, Guan Y, Shang Y Y 2010 *Graphical Models* **72**(1) 1-6
- [14] Li J C, Yang L, Zhong Y-E, Xie C 2012 *Communications in Computer and Information Science* **289** 359-67

Author



Juncheng Li

Current position, grades: Hunan University of Humanities, Science and Technology (China); Lecturer

Scientific interest: Computer aided geometric design and image processing; Information and Computational Science